

# Modeling of CNTs and CNT–Matrix Interfaces in Continuum-Based Simulations for Composite Design

Sanghun Lee, Keesam Shin and Woong Lee<sup>†</sup>

School of Nano & Advanced Materials Engineering, Changwon National University 9 Sarim-dong,  
Changwon, Gyeongnam 641-773, Republic of Korea

(Received July 23, 2010 : Received in revised form August 31, 2010 : Accepted August 31, 2010)

**Abstract** A series of molecular dynamic (MD), finite element (FE) and *ab initio* simulations are carried out to establish suitable modeling schemes for the continuum-based analysis of aluminum matrix nanocomposites reinforced with carbon nanotubes (CNTs). From a comparison of the MD with FE models and inferences based on bond structures and electron distributions, we propose that the effective thickness of a CNT wall for its continuum representation should be related to the graphitic inter-planar spacing of 3.4 Å. We also show that shell element representation of a CNT structure in the FE models properly simulated the carbon-carbon covalent bonding and long-range interactions in terms of the load-displacement behaviors. Estimation of the effective interfacial elastic properties by *ab initio* simulations showed that the in-plane interfacial bond strength is negligibly weaker than the normal counterpart due to the nature of the weak secondary bonding at the CNT-Al interface. Therefore, we suggest that a third-phase solid element representation of the CNT-Al interface in nanocomposites is not physically meaningful and that spring or bar element representation of the weak interfacial bonding would be more appropriate as in the cases of polymer matrix counterparts. The possibility of treating the interface as a simply contacted phase boundary is also discussed.

**Key words** carbon nanotube, molecular dynamic simulation; *ab initio* simulation; nanocomposite.

## 1. Introduction

Since the discovery of carbon nanotubes (CNTs), attentions have been drawn on their superior mechanical and thermal properties for potential applications to novel structural materials. Because individual CNTs are too small to find practical applications to the structural materials, attempts have been made to incorporate them as reinforcements in nanocomposites to fully exploit their high strength and elastic modulus.<sup>1-5)</sup> Composite materials can be prepared to have tailored properties by suitable choices of component systems and their relative proportions. Therefore, it is desirable to design composite systems by modeling and simulation in advance of their productions. Considering the molecular structure of CNTs consisting of carbon walls formed by rolled-up graphene sheets and the cross-sectional dimensions of CNTs in a nanometer order, it is not straightforward to apply typical continuum-based approaches such as representative volume element (RVE) method based on finite element (FE) analysis to predict effective properties of nanocomposites.<sup>6,7)</sup> In order to model CNTs in an FE analysis, it is necessary to define the ‘effective thickness’ of the carbon wall. In addition, since the wall consists of a single carbon layer having in-plane

*sp*<sup>2</sup> hybrid and out-of-plane delocalized *p*<sub>z</sub> orbitals, interfacial region between the CNT and the matrix cannot be clearly defined at the atomistic scale. This may necessitate the definition of ‘interfacial region’ in the continuum model that reflects the characteristic of bonding between CNTs and matrices, especially in case of polymer matrix nanocomposites.<sup>7,8)</sup>

Concerning the effective thickness of carbon walls in CNTs, theoretically estimated values range from 0.7 to 7 Å, reflecting there is no generally accepted value yet.<sup>9-15)</sup> As for the interfacial properties, some works are available on the CNT-polymer interfaces<sup>6-8)</sup> but those on CNT-metal systems are rare despite of the growing importance of metal matrix nanocomposites due to superior wear resistance and high-temperature stabilities as compared to polymer matrix counterparts. Hence, in this study, MD simulation was carried out in combination with FE analysis to estimate ‘proper’ effective thickness of carbon walls in CNTs. Following this, *ab initio* simulation was carried out to verify the necessity of defining interfacial region in continuum-based simulations for composite design by estimating the ‘virtual elastic properties’ of the interfacial region in a CNT-Al system.

## 2. Numerical Analysis

For the estimation of the effective thickness of CNT

<sup>†</sup>Corresponding author

E-Mail : woonglee@changwon.ac.kr (W. Lee)

wall, MD simulations and FE analyses were carried out in parallel. First, uniaxial tension, cantilevered bending and torsion were applied to a model (10,0) CNT in MD separately. The displacements of individual carbon atoms constituting the model CNT were traced with the deformations of CNTs under these simulated loadings. In order to simulate the carbon-carbon bonding, Tersoff potential<sup>16)</sup> was applied. Subsequently, a model CNT was constructed for FE analysis using 8-node thick shell elements for the simplicity purpose (the use of shell elements is justified in following section). The same types of loadings as were used in the MD were applied in the FE analysis with identical magnitudes. Meshing was carried out such that the node points coincide with the positions of carbon atoms in the MD model as shown in Fig. 1 and the elastic modulus was taken to be 1.0 TPa, a most agreed value.<sup>17)</sup> FE analyses were repeated with varying shell thickness until the overall deformation of the shell model becomes identical to that predicted from the MD simulation under the same load. In this manner, the effective carbon wall

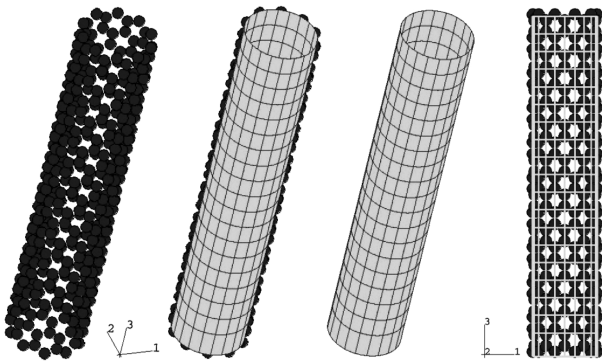


Fig. 1. MD model and corresponding FE model of a (10,0) CNT employed as a model system for the simulations.

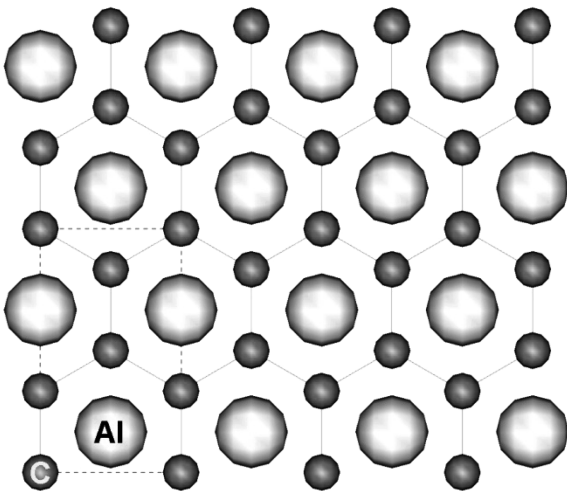


Fig. 2. Arrangement of atoms at the interface between a graphene sheet and an Al (111) layer used in the *ab initio* simulation.

thickness was determined by the shell thickness that yielded the identical shape deformations in both the simulations.

For the characterization of the CNT–Al interfaces, ‘stiffnesses’ of the interfacial bonding was estimated along the normal and lateral directions with respect to the plane of interface by *ab initio* simulations. Nothing that the Al (111) plane can be matched to the graphene layer, coherent interface was assumed as shown in the interface registry in Fig. 2. Bonding stiffnesses were calculated from the dispersion relations obtained for the graphene–Al systems. Calculations were carried out within the framework of density functional theory (DFT) in which the local density approximation (LDA) is implemented based on a plane wave basis set and separable Troullier–Martins-type pseudopotentials.<sup>18)</sup>

### 3. Results and Discussion

In Figs. 2 and 3, the changes in shapes of the MD model and those of the FE model under the same loading condition are compared for tension, bending and torsion, respectively. It is clearly seen that not only the overall deformed shapes predicted by two simulations agree well with each other but the displaced nodal points in the deformed FE meshes correspond with the displaced atomic positions in the loaded MD models. The shell thicknesses that yielded such symmetries in deformations were 2.1 Å for the uniaxial tension and 3.6 Å for the bending and the torsion. These values are comparable to the known value of the graphitic inter-planar spacing of 3.4 Å and in this sense they are not much different from the values of 5 to 7 Å predicted in the previous work where FE analysis employed a CNT model represented by truss-and-spring elements.<sup>15)</sup> This result also supports the suggestion that the previously accepted value of 0.7 Å is not suitable for the application to continuum models of CNTs in numerical calculations.<sup>15,19)</sup> Further, it should be noted that the truss-and-spring model considered the deformation of a unit cell, *viz.* the basic repeating unit whereas the model in the current study considered the structural deformation of a whole CNT geometry as well as the displacements of individual carbon atoms. Accordingly, there is a possibility that the use of truss-and-spring elements for the continuum representation of CNT structure underestimated the structural ‘stiffness’ of the CNTs. It is thus believed that the wall thickness derived in this study would be more realistic since the whole geometry is usually considered in a continuum modeling.

As regarding the effective thickness of the CNT walls, it would also be instructive to consider the van der Waals radius of carbon, which is known to be 1.7 Å. Since the graphene sheet consists of covalently bonded in-plane carbon atoms and delocalized sea of electrons from out-of-plane  $p_z$  orbitals responsible for weak secondary bonding

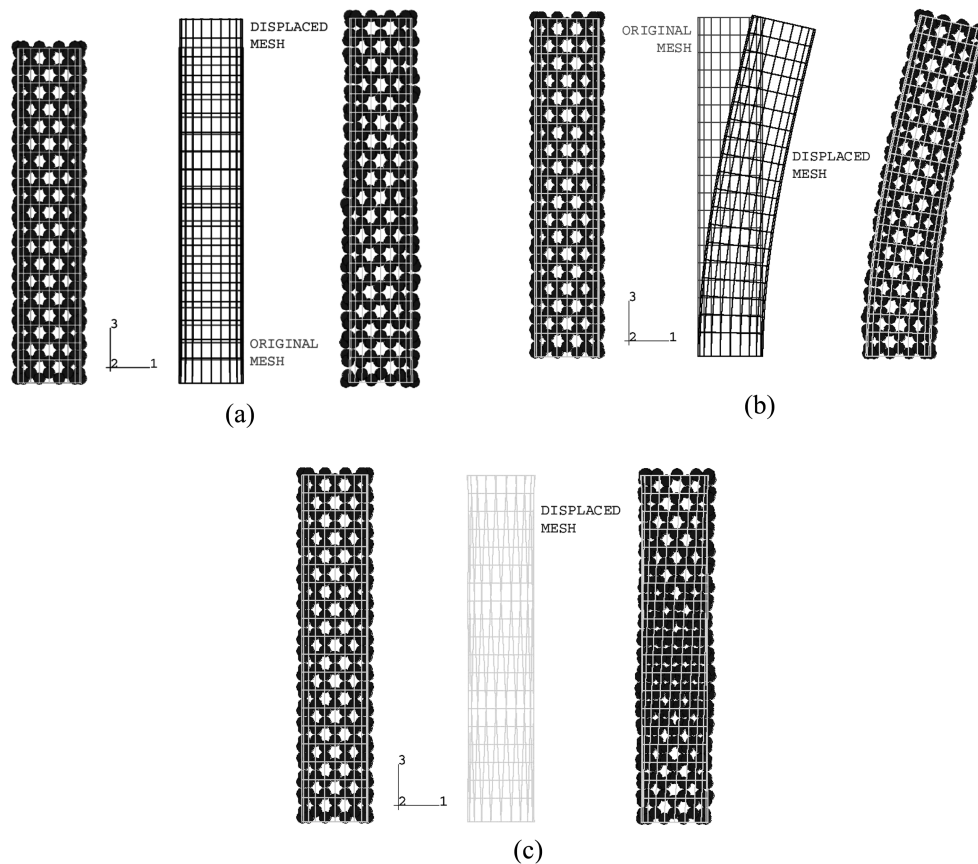


**Fig. 3.** Comparison of the displacement of atomic positions in MD model with the nodal displacements in corresponding FE model under (a) uniaxial tension, (b) cantilevered bending and (c) torsion.

with other species, it would be natural to consider the effective thickness in terms of the range of the van der Waals radius. Further, in a previous work on the interaction between a graphene sheet and an Al (111) layer at a coherent interface, the inter-species equilibrium distance was estimated to be about 3.84 Å while the interaction is predicted to be a weak secondary type related to van der Waals bonding.<sup>20)</sup> Noting that the van der Waals radius of an Al atom is 1.84 Å, the equilibrium bonding distance of 3.84 Å seems to be closely related to the numerical sum of the van der Waals radii of carbon and aluminum, which is 3.54 Å. If the wall thickness is taken to be 5 to 7 Å as predicted by the truss-and-spring CNT model in a previous work,<sup>15)</sup> it would indicate that the bonding between two species results in substantial overlapping of 'hard' graphitic layer and 'hard' Al layer violating the structural equilibrium.<sup>17)</sup> This situation is then similar to the severe deformation of atomic 'hard spheres' in typical chemical bonding in solids, which is obviously not the case.

One may choose the effective wall thickness as 0.7 Å instead. However, this value is substantially smaller than the carbon-carbon covalent bond length of 1.42 Å. Since bonding between a CNT and a matrix is usually of

secondary long-range type, use of such effective thickness smaller than the covalent bond length leaves significant interior gap in the interfacial region causing difficulty in continuum elastic model.<sup>19)</sup> Therefore, if any judgment on the effective thickness is to be made, it would be reasonable to base on the extent of the electron 'clouds' of constituent species. In this respect, use of the values of 2.1 and 3.6 Å (the actual value dependent on the specific loading condition) estimated in this study or inter-planar spacing of 3.4 Å would be more realistic in continuum modeling of CNT-reinforced nanocomposites.

The deformed FE mesh shapes that correspond well with the atomic displacements in MD model have practical implication. Despite of representing the nanostructure having atomistic dimensions as a continuous shell, the FE model could simulate the inter-atomic bonding stiffness between the adjacent carbon atoms as well as the long range interaction among remote carbon atoms in that the nodal displacements agree well with the atomic displacements. If the carbon-carbon bonding is modeled with truss and spring elements, the FE model becomes inevitably complicated and therefore the calculation can be limited to the 'unit cell' or small portion of CNTs alone as in the case of

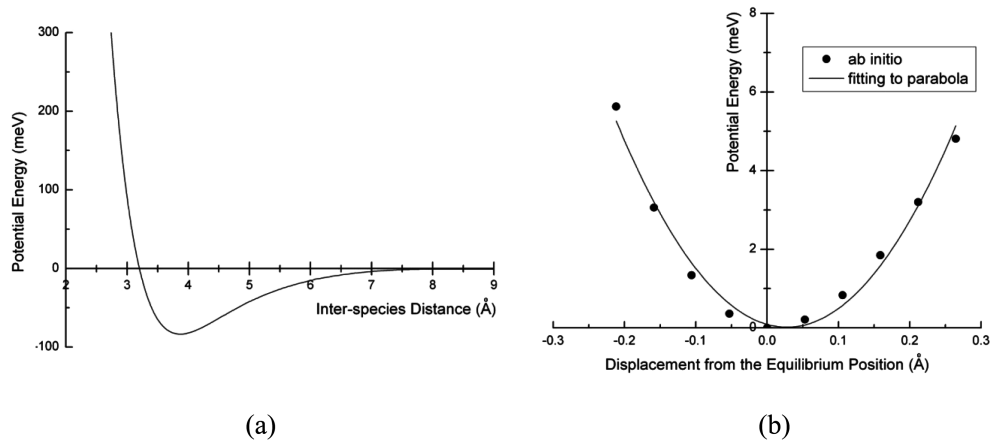


**Fig. 4.** (a) Changes in the inter-species potential energy with the approach of Al (111) layer toward the graphene layer and (b) harmonic potential approximation of the inter-species potential energy in the vicinity of the equilibrium point.

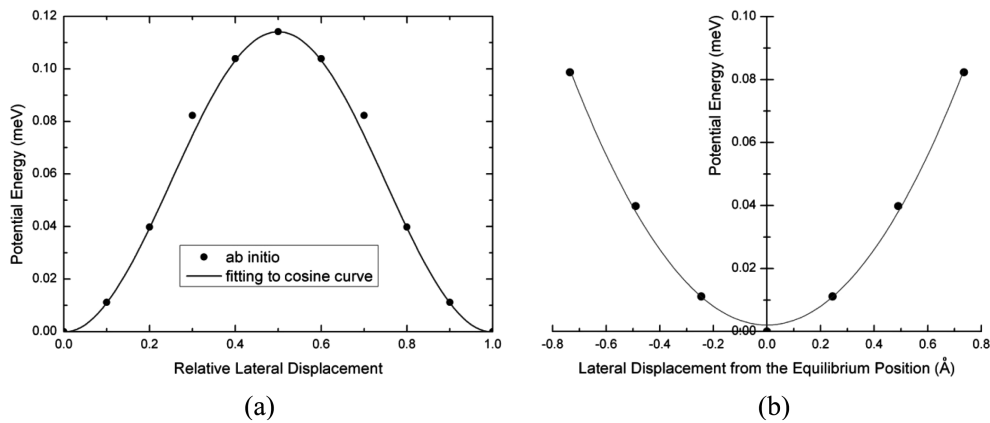


**Fig. 5.** (a) Changes in the inter-species potential energy with the translation of Al (111) layer over the graphene layer and (b) harmonic potential approximation of the inter-species potential energy in the vicinity of the equilibrium point.

the previous work.<sup>15)</sup> Instead of the truss and spring representations, it is possible to employ full three dimensional solid elements (brick elements) to model CNTs. In such a case, however, since more than one element should be used along the radial direction to ensure numerical accuracy,<sup>21)</sup> meshing size can be larger compared with shell elements, resulting in increase computational costs. Therefore, it is suggested that use of shell elements for modeling CNT walls in continuum calculations can be a computationally efficient approach.

Having defined the effective thickness of the CNT wall, the effective mechanical properties of the interfacial region in a model CNT–Al nanocomposite is now investigated. Fig. 4(a) shows the changes in inter-species potential energy with respect to the separation distance represented as an averaged pair-wise sum on all particles in a unit cell (refer to Fig. 2 for unit cell registry). It is seen that the dispersive relation is similar to that for typical long-range inter-species interactions while the cohesive energy is about 84 meV and the equilibrium separation distance is

about 3.84 Å. These values are typical of weak long-range interaction such as van der Waals bond, supporting the discussion on the effective CNT wall thickness based on the van der Waals radii of constituent species. Further, it is noticed in Fig. 4(b), which is the reproduction of the energy profiles near the equilibrium point, that the dispersive relation can reasonably be fitted to a parabola, *i.e.* it can be approximated as a harmonic potential. From the second derivative of the harmonic potential representation of the potential energy curve in Fig. 4(b), effective elastic modulus of the interfacial region along the direction normal to the interface can be estimated, which is about 15.3 GPa.

In addition to the potential energy variation along the normal direction, that along the in-plane direction was also calculated to estimate the shear property of the interface region. Fig. 5(a) shows how the inter-species potential undergoes a change while Al (111) plane is translated over the graphene sheet along  $[1\bar{1}0]$  direction from an equilibrium position to the adjacent one. It is seen that the

changes in the potential energy along the  $[1\bar{1}0]$  direction can be represented as a cosine function, which is an indication that the translational motion of the Al (111) plane over a graphene layer can be represented by a slip motion of an atomic plane in perfect lattice. Again, the potential energy curve in the vicinity of the equilibrium point can be fitted to a harmonic potential as shown in Fig. 5(b) and the shear modulus estimated from its second derivative is about 25.1 MPa.

The estimated elastic and shear moduli of 15.3 GPa and 25.1 MPa respectively gives physically unacceptable Poisson's ratio which should be in the order of  $10^3$ . Therefore, it is not possible to model the interfacial region with typical solid element in FE analysis as a third-phase region, although the effective elastic and shear moduli are estimated. It would then be more appropriate to use such element as spring or bar elements to simulate weak interfacial bonding as has been applied to polymer matrix nanocomposites.<sup>7,8)</sup> Alternatively, since the interfacial region has negligible thickness after considering the effective CNT wall thickness and the Al (111) layer thickness, it would be possible to treat the interface as a phase boundary as in the case of typical composite systems.<sup>21)</sup> More work would be needed both experimentally and theoretically to investigate this further.

#### 4. Conclusion

Series of MD simulations and FE analysis carried out in parallel indicated that the effective thickness of a CNT wall is closely related to the graphitic inter-planar distance of 3.4 Å while the exact values are dependent on the loading conditions. The estimated values were also correlated reasonably to the 'virtual' thickness of the wall inferred from the van der Waals radius of carbon. Since the deformed FE model, which simulates the CNT structure with continuum shell, reflected the atom by atom deformation of the CNT in MD model in terms of the nodal displacements in addition to the overall deformations correctly, it is inferred that shell modeling of the CNT is suitable for continuum-based analysis and design of CNT-reinforced nanocomposites. In *ab initio* simulations, the estimated elastic properties of the interfacial region based on the inter-species interaction potential profiles indicated that the modeling of the interfacial region as a third-phase region with solid elements is not suitable for simulating physically acceptable mechanical behaviors. It is proposed that the use of spring or bar representation for the inter-species interaction at the interface or the phase boundary treatment of the interface would be more appropriate.

#### Acknowledgement

This work was supported by the Korea Research Foundation Grant funded by the Korean Government (KRF-2008-313-D00485) (S. Lee and W. Lee) and Changwon National University (K. Shin and W. Lee).

#### References

1. Y. -K. Choi, K. Sugimoto, S. -M. Sing, Y. Gotoh, Y. Ohkoshi and M. Endo, *Carbon*, **43**, 2199 (2005).
2. S. Rul, F. Lefèvre-schlick, E. Capria, Ch. Laurent and A. Peigney, *Acta Mater.*, **52**, 1061 (2004).
3. R. Zhong, H. Cong and P. Hou, *Carbon*, **41**, 848 (2003).
4. L. Wang, H. Choi, J.-M. Myoung and W. Lee, *Carbon*, **47**, 3427 (2009).
5. S. Kim, H. Lee, J. Kim, C. S. Son and D. Kim, *Kor. J. Mater. Res.*, **20**(1), 25 (2010) (in Korean).
6. Y. J. Liu and X. L. Chen, *Mech. Mater.*, **35**, 69 (2003).
7. S. A. Meguid, J. M. Wernik and Z. Q. Cheng, *Int. J. Solid. Struct.*, **47**, 1723 (2010).
8. C. Y. Li and T. S. Chou, *Compos. Sci. Tech.*, **66**, 2409 (2006).
9. B. I. Yakobson, C. J. Brabec and J. Bernholc, *Phys. Rev. Lett.*, **76**, 2511 (1996).
10. X. Zhou, J. J. Zhou and Z. C. Ou-Yang, *Phys. Rev. B*, **62**, 13692 (2000).
11. J. P. Lu, *Phys. Rev. Lett.*, **79**, 1297 (1997).
12. K. N. Kudin, G. E. Scuseria and B. I. Yakobson, *Phys. Rev. B*, **64**, 235406 (2001).
13. C. Li and T. -W. Chou, *Int. J. Solid. Struct.*, **40**, 2487 (2003).
14. K. I. Tserpesa and P. Papanikos, *Compos. B Eng.*, **36**, 468 (2005).
15. G. M. Odegard, T. S. Gates, L. M. Nicholson and K. E. Wise, *Compos. Sci. Tech.*, **62**, 1869 (2002).
16. J. Tersoff, *Phys. Rev. B*, **37**, 6991 (1988).
17. T. Vodenticharova and L. C. Zhang, *Phys. Rev. B*, **68**, 165401 (2003).
18. N. Troullier and J. L. Martins, *Phys. Rev. B*, **43**, 1993 (1991).
19. C. Q. Ru, *Phys. Rev. B*, **62**, 9973 (2000).
20. W. Lee, S. Jang, M. J. Kim and J. -M. Myoung, *Nanotechnology*, **19**, 285701 (2008).
21. R. D. Cook, *Finite Element Modeling for Stress Analysis*, p. 105-144, John Wiley & Sons, NY, USA (1995).
22. A. Haque and A. Ramasetty, *Compos. Struct.*, **71**, 68 (2005).